

Shock Tube and Modeling Study of the Monomethylamine Oxidation at High Temperature

Kuan Soo Shin* and Sang Jo Yoo

Department of Chemistry, Soongsil University, Seoul 156-743, Korea

Received October 30, 2003

The ignition of monomethylamine was studied in reflected shock waves over the temperature range of 1255-1579 K and the pressure range of 1.04-1.51 bar. The ignition delay time was measured by the sudden increase of pressure profile and the radiation emitted by OH radicals. The relationship between the ignition delay time and the concentrations of monomethylamine and oxygen was determined in the form of mass-action expressions with an Arrhenius temperature dependence. In contrast to the behavior observed in hydrocarbons, monomethylamine acts to accelerate rather than inhibit its own ignition. And numerical modeling of the ignition of CH_3NH_2 has also been carried out to test the several kinetic mechanisms.

Key Words : Monomethylamine, Ignition, Shock tube, Nitrogen oxides

Introduction

Nitrogen-containing fuels are responsible for a significant part of NO emissions from practical combustion systems. The problem of NO formation from fuel nitrogen becomes particularly important for the incineration of nitrogen-containing materials. Incineration of the nitrogen-containing compound will produce oxides of nitrogen such as NO, NO_2 , and possibly N_2O . The nitrogen oxides contribute to the formation of photochemical smog, and N_2O depletes ozone in the stratosphere and is a greenhouse gas. NO is known to be formed in a variety of ways: (1) "Thermal NO" (Zeldovich, 1946)¹ is primarily a consequence of high flame temperatures; (2) "Prompt NO" (Fenimore, 1976)² is generated in fuel-rich parts of flames; (3) the " N_2O mechanism" (Wolfrum, 1972³; Malte and Pratt, 1974⁴) can be important in high-pressure flames; (4) "Fuel NO" (Fenimore, 1976)² results from converting nitrogen-containing compounds in the fuel into NO; and (5) the NNH mechanism (Bozzelli and Dean, 1995)⁵ is active in flame fronts where high atom concentrations appear.

There are several methods for the reduction of nitrogen oxides formed as unwanted by-products in technical combustion processes called the selective catalytic reduction (SCR) and selective non-catalytic reduction (SNCR) methods. In SNCR systems, ammonia (Thermal DeNO_x),⁶ urea (NO_xOUT),⁷ and cyanuric acid (RaprNO_x)⁸ are used as reductants. In these processes, NO removal occurs through a reaction with NH_2 radical, which is derived from SNCR agents through reaction with OH and O. Since these methods can only be generated at temperatures over 1000 K, NO reduction is difficult at temperatures below 1000 K.⁹ Monomethylamine (CH_3NH_2) is an alternative substance producing NH_2 radicals in the thermal decomposition and, it could be used for the reduction of NO.¹⁰ Because the derivation of NH_2 from amines begins at temperatures around 600 K,¹¹

The high temperature pyrolysis of monomethylamine has

been investigated by Higashihara *et al.*¹² Klatt *et al.*¹³ and Votsmeier *et al.*¹⁴ using various shock tube techniques. Higashihara *et al.*¹² was studied by IR laser kinetic absorption spectroscopy behind reflected shock waves with over the temperature range from 1400 K to 1820 K. Klatt *et al.*¹³ studied the decomposition of monomethylamine behind incident shock waves in the temperature range from 1750 K to 2450 K. Recently, Votsmeier *et al.*¹⁴ studied thermal decomposition of monomethylamine using laser absorption diagnostic and kinetic shock tube studies. They measured NH_2 radical concentration profiles with sensitive laser absorption diagnostic for NH_2 at a detection wavelength of 16739.90 cm^{-1} and computationally simulated with detailed kinetics. In contrast with the monomethylamine pyrolysis, the monomethylamine oxidation behind shock waves, however, was not much studied experimentally except for Hwang *et al.*¹⁵ and Lifshitz *et al.*¹⁶ Hwang *et al.*¹⁵ studied monomethylamine oxidation by IR laser kinetic absorption spectroscopy behind reflected shock waves over the temperature range 1260-1600 K and modeled with a 141 reaction mechanism. Lifshitz *et al.*¹⁶ studied the ignition of monomethylamine in reflected shock waves over the temperature range from 1000 to 1300 K. Katak *et al.*¹⁷ recently studied the oxidation of monomethylamine in a flow reactor over the temperature range of 600-1400 K and assembled a reaction mechanism describing the monomethylamine conversion under these conditions.

Monomethylamine as the simplest primary organic amine is the model compound to study the 'Fuel NO' mechanism converting nitrogen-containing fuel to NO and it also acts as an SNCR agent by producing NH_2 radical to reduce NO. In order to understand more details of the role of monomethylamine under combustion environment, more experimental and modeling studies are needed. In this investigation, the ignition delay times of $\text{CH}_3\text{NH}_2\text{-O}_2\text{-Ar}$ mixtures were measured over the temperature range from 1255 K to 1579 K, and a correlation between ignition delay times and concentrations of CH_3NH_2 and O_2 was investigated. Several kinetic mecha-

nisms for CH_3NH_2 oxidation at high temperature have also been tested by the computer simulation.

Experimental Section

The experiments were performed behind reflected shock waves in stainless-steel shock tube which was described in detailed elsewhere.²⁴⁻²⁶ The apparatus consists of a 514 cm (6.02 cm i.d.) 304 stainless-steel tube separated from the He driver gas chamber by a unscored aluminium diaphragm with 0.1 mm thickness. The tube is routinely pumped between experiments to $< 10^{-7}$ torr by turbo molecular pump (Varian, 969-9002) system. The velocity of the shock wave was measured with five pressure transducers (PCB 113A21) connected to four digital timer/counters (Fluke PM6666). The temperature and pressure in the reflected shock wave regime were calculated from this velocity.²⁴⁻²⁶

The ignition was measured by the sudden increase of pressure profile and OH emission intensity. The pressure measurements were made using a pressure transducer (PCB 113A21) which was located at 1.0 cm from the reflecting surface. The characteristic ultraviolet emission from OH radical species at 306.7 nm was monitored using a photomultiplier tube (ARC DA-781) with a band path filter (Andover, 308 nm) through the sapphire window which was mounted flush at 1.0 cm from the end plate of shock tube. The window was masked to 1 mm slit width in order to reduce emission intensity and improve the time resolution of the system. Both traces were fed into a digital oscilloscope (HP 45601A).

The compositions of the mixtures are given in Table 1. The equivalence ratio was varied to examine the composition dependences on the ignition delay time. CH_3NH_2 (98%, Aldrich), O_2 (99.99%, Dongmin) and Ar (99.9993%, Donga) were used without further purification. He (99.9995%, Dongmin) was used as a driver gas. Test gas mixtures were prepared manometrically and then used after keeping for over 24 hours in aluminium cylinders. The initial pressure (P_1) was fixed to 30 torr and the shock velocity could be controlled by changing the pressure of He driver gas. The measurements covered a temperature range (T_5) of 1255-1579 K and a pressure range (P_5) of 1.04-1.51 bar behind reflected shock waves. The measured ignition delay times ranged from 66 to 1373 μs .

Table 1. The experimental conditions for $\text{CH}_3\text{NH}_2\text{-O}_2\text{-Ar}$ mixtures

	Compositions (%)			τ (μsec)	T_5 (K)	P_5 (bar)
	CH_3NH_2	O_2	Ar			
Mixture 1	2.0	5.5	92.5	66-781	1324-1538	1.13-1.44
Mixture 2	2.0	2.8	95.2	110-816	1390-1579	1.18-1.45
Mixture 3	1.0	5.5	93.5	138-1137	1321-1488	1.04-1.27
Mixture 4	2.0	11.0	87.0	76-1373	1255-1486	1.07-1.45
Mixture 5	4.0	5.5	90.5	101-1230	1282-1475	1.19-1.51
Mixture 6	3.0	8.3	88.7	85-844	1288-1485	1.15-1.48

Results and Discussion

Figure 1 shows a typical oscilloscope trace for pressure and OH emission profiles measured at 1.0 cm from the reflecting end plate. The upper trace records the total pressure and the lower trace the OH emission. The ignition delay time (τ) was defined as the time interval between the arrival of the reflected shock wave front and the onset of an ignition. The ignition delay time derived from the OH emission is almost the same as that derived from the pressure profile. The effects of CH_3NH_2 and O_2 concentrations on the ignition delays are shown in Figure 2.

A correlation between ignition delays and concentrations was customarily summarized in the form of mass-action expressions with an Arrhenius temperature dependence.²⁷ Multiple regression analysis was employed to obtain the best-fit parameters. This procedure gave

$$\tau = 6.29 \times 10^{-12} \exp(44 \text{ kcal mol}^{-1}/RT) \times [\text{CH}_3\text{NH}_2]^{-0.23} [\text{O}_2]^{-0.86}$$

where τ and the concentrations are given in sec and mol/cm^3 ,

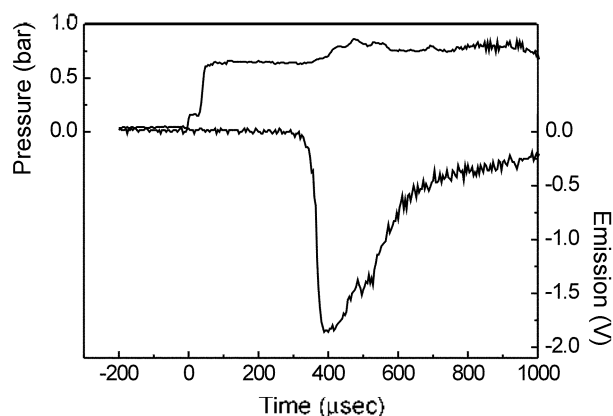


Figure 1. Typical experimental record showing pressure (upper) and OH emission (lower). Experimental conditions were $P_1 = 30$ torr, $P_5 = 1.33$ bar, and $T_5 = 1425$ K in mixture 4.

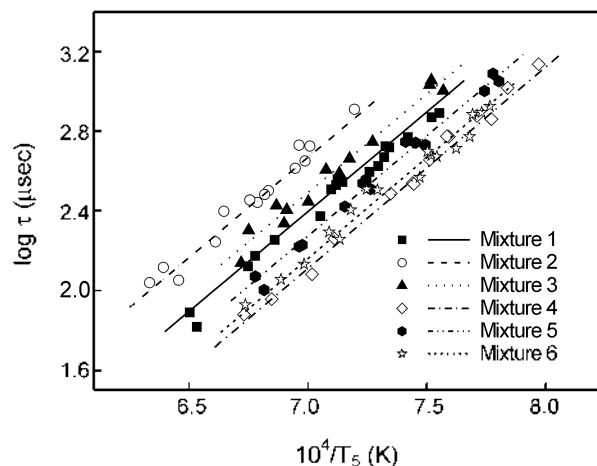


Figure 2. Ignition delay times for the mixtures shown in Table 2. Lines represent the least squares fits for the corresponding mixtures using the expression in the text.

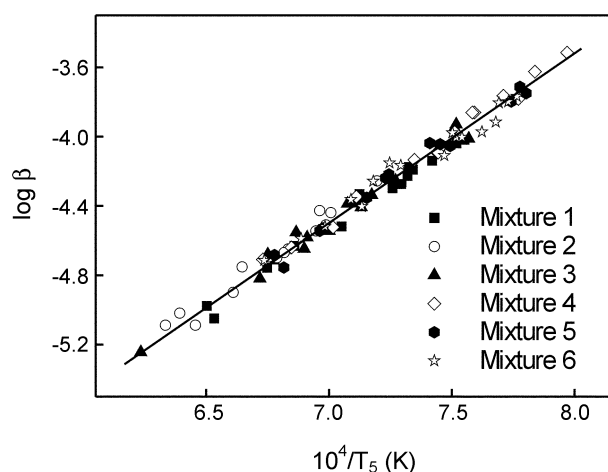


Figure 3. A plot of $\log \beta$ vs. $10^4/T_5$ for all mixtures; $\beta = \tau \{[\text{CH}_3\text{NH}_2]^{-0.23}[\text{O}_2]^{0.86}\}$.

respectively. It is worth noting that the parameters are valid only for the specific ranges of pressure, temperature and concentrations over which ignition delays were measured. The reliability of this empirical formula was tested by plotting all data as $\log(\tau \{[\text{CH}_3\text{NH}_2]^{-0.23}[\text{O}_2]^{0.86}\})$ vs. $10^4/T_5$. As shown in Figure 3, all points lie close to a single line. The power dependence of monomethylamine indicates self-accelerating effect; the ignition delay times decrease by increasing the concentration of monomethylamine. And, the power dependence of oxygen indicates the promotion effect; the ignition delay times decrease by increasing the concentration of oxygen. In this investigation, the argon dependence on the ignition of monomethylamine was not obtained because the concentration of argon in our mixtures was not varied much.

At first glance, CH_3NH_2 would be expected to ignite in a manner analogous to ethane (C_2H_6). Both decompose thermally by central bond breaking to form relatively unreactive radicals and both yield radicals upon H-abstraction that decompose to H-atoms and more slowly igniting species, C_2H_4 and CH_2NH . In fact, CH_3NH_2 and C_2H_6 ignite differently. The power dependence of the ignition delay on the small hydrocarbon concentration is usually positive.²⁸⁻³⁰ It indicates that the hydrocarbon fuel inhibits the ignition process. For most hydrocarbon fuels (RH), the reaction $\text{H} + \text{RH} \rightarrow \text{H}_2 + \text{R}$ competes with chain branching reaction $\text{H} + \text{O}_2 \rightarrow \text{OH} + \text{O}$ for hydrogen atoms and is responsible for the positive power dependence on fuel concentration. In contrast with small hydrocarbons, the power dependence of ignition delay on CH_3NH_2 concentration shows negative dependence (-0.23), which means that CH_3NH_2 itself has the promotion effect in the ignition process.

In order to understand more details on monomethylamine oxidation at high temperature, the numerical modeling study was also tested using various reaction mechanisms. The reaction mechanism of CH_3NH_2 oxidation usually could be divided into three parts; (1) the first part of the mechanism is mainly composed of the initial reactions concerning the CH_3NH_2 consumption, (2) the second part is constructed

Table 2. Mechanisms for the oxidation of monomethylamine at high temperature

Mechanism	No. of reactions	No. of species
Mechanism 1: Kantak <i>et al.</i> ¹⁷	65	350
Mechanism 2: Hwang <i>et al.</i> ¹⁵	44	141
Mechanism 3: GRI 3.0 ¹⁸ + Hwang <i>et al.</i> ¹⁵	59	371
Mechanism 4: Kantak <i>et al.</i> ¹⁷ – Dean & Bozzelli ²⁰	65	350
Mechanism 5: Dean & Bozzelli ²⁰ + GRI 3.0 ¹⁸	73	424
Mechanism 6: Coda <i>et al.</i> ¹⁹ + Dean & Bozzelli ²⁰	64	410

using NO formation and destruction reactions, (3) the rest part of the mechanism is consisted of hydrocarbon oxidation reactions concerning the C_1 or C_2 hydrocarbon species. The mechanisms used in this modeling study of monomethylamine oxidation are listed in Table 2. The reaction mechanism proposed by Hwang *et al.*¹⁵ consists of 141 elementary reactions with 44 species. Kantak *et al.*¹⁷ also reported their mechanism composed of 350 elementary reactions and 65 species. In mechanism 3, a large set of reactions describing C_1 and C_2 hydrocarbon and NO chemistry was taken from the GRI 3.0 mechanism¹⁸ and the CH_3NH_2 reactions were taken from a mechanism proposed by Hwang *et al.*¹⁵ The mechanism proposed by Coda *et al.*¹⁹ involves 57 species in 353 elementary gas-phase reactions. In Coda *et al.*¹⁹ mechanism, the oxidation reactions of C_1/C_2 hydrocarbons, HCN, and NH_3 , as well as the reactions between hydrocarbons (CH_i , HCCO) and nitrogen species (NO , NH_i , N_2) were included. Dean and Bozzelli²⁰ recently reviewed the reactions involving nitrogen species. In order to construct the CH_3NH_2 consumption submechanism, 65 elementary reactions were taken from Dean and Bozzelli²⁰ mechanism in the mechanisms 4, 5 and 6 in Table 2.

Computations of modeling were carried out using Sandia Chemkin III code.²² Thermodynamic data were obtained from Chemkin thermodynamic data base.²¹ The rate constants for the reverse reactions were calculated with the forward rate constants and the appropriate equilibrium constants. As shown in Figure 4, the calculated ignition delay times using the mechanism 6 (Coda *et al.*¹⁹ + Dean and Bozzelli²⁰), which consists of 410 elementary reactions with 64 species, shows the best agreement with the observed ones for all mixtures.

In the complex reaction mechanism, all of elementary reactions do not contribute equally to the ignition delay times of monomethylamine, but some of them may do essentially. In order to find the sensitive reactions, logarithmic sensitivity analysis,³¹ listed in Table 3, was calculated using the mechanism 6. Sensitivity analysis was performed on all reactions by increasing forward rate constant, multiplying a rate constant by factor of 2,

$$S_{ij} = \frac{\Delta \log \tau_i}{\Delta \log k_j}$$

where, τ_i is ignition delay time at condition of i . And k_j is rate constant of j the elementary reaction. S_{ij} is logarithmic

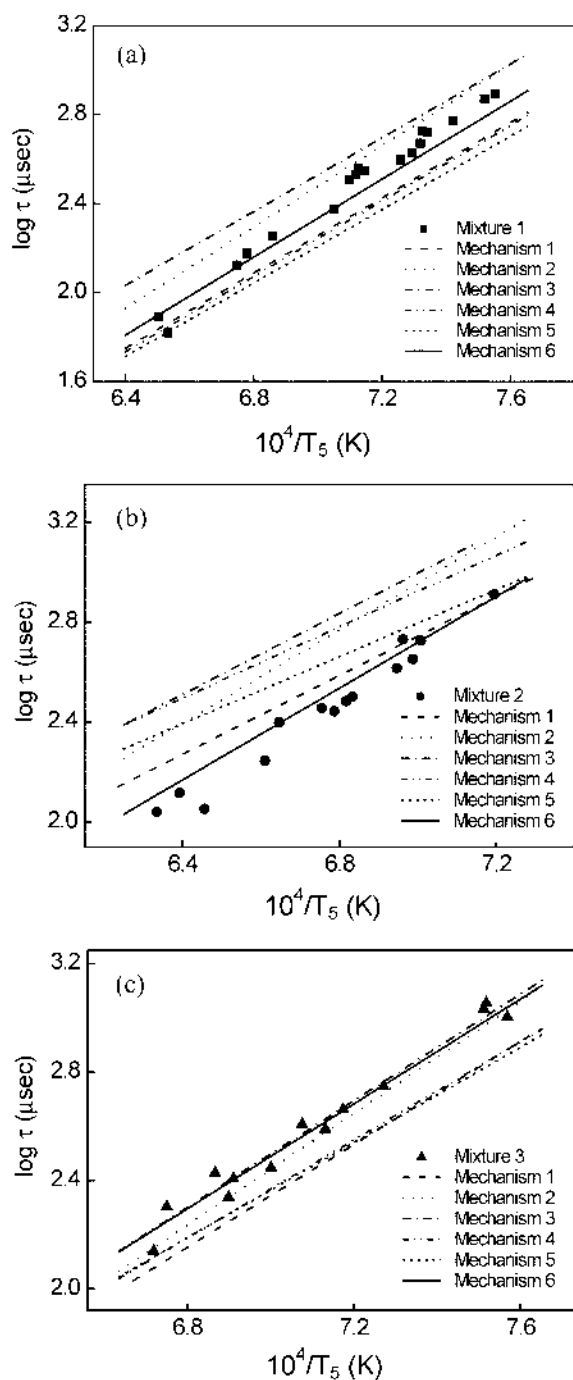
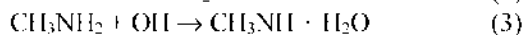
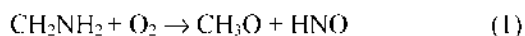


Figure 4. Comparison of observed ignition delay times (symbols) with calculated ones (lines) using the CH_3NH_2 oxidation mechanisms. (a) mixture 1 (near stoichiometric), (b) mixture 2 (fuel rich), (c) mixture 3 (fuel lean).

sensitivity. The sensitivity analysis shows the following reactions are important in the ignition of CH_3NH_2 .

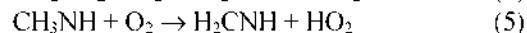


Reactions (1) and (3) are the initiation reactions and reaction (2) is the chain branching reaction. These three reactions are important in the ignition process. As shown in the Table 3.

Table 3. Logarithmic sensitivity values of ignition delay time for mixtures 3 (lean), 1 (stoichiometric), and 5 (rich) at $T_5 = 1400$ K. Sensitivities less than 0.02 are not listed

Reaction	Mixture 3	Mixture 1	Mixture 5
$\text{CH}_2\text{NH}_2 + \text{O}_2 \rightarrow \text{CH}_3\text{O} + \text{HNO}$	-0.29374	-0.22214	-0.16288
$\text{O} + \text{OH} \rightarrow \text{H} + \text{O}_2$	-0.29124	-0.22854	-0.25593
$\text{CH}_3\text{NH}_2 + \text{OH} \rightarrow \text{CH}_3\text{NH} + \text{H}_2\text{O}$	-0.25348	-0.25026	-0.26427
$\text{CH}_2\text{NH}_2 + \text{O}_2 \rightarrow \text{H}_2\text{CNH} + \text{HO}_2$	-0.11116	-0.12241	-0.14309
$\text{CH}_3\text{NH} + \text{O}_2 \rightarrow \text{H}_2\text{CNH} + \text{HO}_2$	-0.08216	-0.11432	-0.16115
$\text{HO}_2 + \text{H} \rightarrow \text{OH} + \text{OH}$	-0.08001	-0.07188	-0.09352
$\text{CH}_2\text{NH}_2 + \text{H}_2\text{O}_2 \rightarrow \text{CH}_3\text{NH}_2 + \text{HO}_2$	-0.07141	-0.10413	-0.13882
$\text{CH}_3\text{NH} + \text{H}_2\text{O}_2 \rightarrow \text{CH}_3\text{NH}_2 + \text{HO}_2$	-0.06927	-0.09613	-0.13117
$\text{NO} + \text{HO}_2 \rightarrow \text{NO}_2 + \text{OH}$	-0.05543	-0.06562	-0.09849
$\text{H}_2\text{NO} + \text{H} \rightarrow \text{NH}_2 + \text{OH}$	-0.04873	-0.06823	-0.10097
$\text{HCNH} + \text{O}_2 \rightarrow \text{HCN} + \text{HO}_2$	-0.04698	-0.08343	-0.14309
$\text{NH}_2 + \text{NO} \rightarrow \text{NNH} + \text{OH}$	-0.04417	-0.04649	-0.06167
$\text{HCO} + \text{O}_2 \rightarrow \text{CO} + \text{HO}_2$	-0.04032	-0.07031	-0.14309
$\text{CH}_3\text{NH}_2 + \text{H} \rightarrow \text{CH}_3\text{NH} + \text{H}_2$	-0.03683	-0.04855	-0.05925
$\text{NH}_3 + \text{OH} \rightarrow \text{NH}_2 + \text{H}_2\text{O}$	0.03226	0.03002	0.05468
$\text{HO}_2 + \text{H} \rightarrow \text{H}_2 + \text{O}_2$	0.03525	0.03343	0.05765
$\text{CH}_3\text{NH}_2 + \text{H} \rightarrow \text{CH}_2\text{NH}_2 + \text{H}_2$	0.04977	0.06372	0.11952
$\text{HO}_2 + \text{OH} \rightarrow \text{H}_2\text{O} + \text{O}_2$	0.08352	0.07131	0.07466
$\text{CH}_3\text{NH} + \text{O}_2 \rightarrow \text{CH}_3\text{O} + \text{HNO}$	0.08448	0.12474	0.17473
$\text{CH}_3\text{NH}_2 + \text{OH} \rightarrow \text{CH}_2\text{NH}_2 + \text{H}_2\text{O}$	0.16913	0.16345	0.18906

however, the special features of the fuel accelerating effect in the ignition of monomethylamine come from the following reactions, the formation reactions of HO_2 and the reaction of $\text{HO}_2 + \text{H} \rightarrow \text{OH} + \text{OH}$.



Formation of HO_2 by H-atom transfers to O_2 , followed by subsequent reaction of HO_2 with H to two OH radicals, are the steps that provide the accelerating effect of monomethylamine.

Conclusions

In the present study, a comprehensive shock tube and modeling investigation was performed on the ignition of $\text{CH}_3\text{NH}_2\text{-O}_2\text{-Ar}$ mixtures in the temperature range of 1255–1579 K and the pressure range of 1.04–1.51 bar. The ignition delay times were measured by the increase of pressure and OH emission. A correlation between ignition delay times and concentrations of monomethylamine and oxygen could be summarized in the following empirical formula.

$$\tau = 6.29 \times 10^{-12} \exp(44 \text{ kcal mol}^{-1}/RT) [\text{CH}_3\text{NH}_2]^{-0.23} [\text{O}_2]^{-0.86} (\text{mol}/\text{cm}^3)^{1.09} \text{ sec}$$

In contrast to the behavior observed in small hydrocarbons, which usually inhibit their own ignition, monomethylamine acts to accelerate rather than inhibit its own ignition. Several kinetic mechanisms proposed for monomethylamine oxidation at high temperatures have been

tested by the computer simulation. It was found that the ignition delay times calculated from the mechanism 6 in Table 2 were in good agreement with our experimental data. A model study showed that the formation reactions of HO₂ followed by the reaction of HO₂ + H → OH + OH are the steps that provide the accelerating effect of monomethylamine.

Acknowledgment. This work was supported by the Soongsil University Research Fund.

References

1. Zeldovich, Y. B. *Acta Physicochimica U.R.S.S.* **1946**, *21*, 577.
2. Fenimore, C. P. *Combustion and Flame* **1976**, *26*, 249.
3. Wolfrum, J. *Chemie Ingenieur Technik* **1972**, *44*, 656.
4. Malte, P. C.; Pratt, D. T. *Combust. Sci. Tech.* **1974**, *9*, 221.
5. Bozzelli, J. W.; Dean, A. M. *Int. J. Chem. Kinet.* **1995**, *27*, 1097.
6. Miller, J. A.; Branch, M. C.; Kee, R. J. *Combustion and Flame* **1981**, *43*, 81.
7. Arand, J. K.; Muzio, L. J.; Sotter, J. G. *U. S. Patent 4* **1982**, 208, 386.
8. Carton, J. A.; Siebers, D. L. *ASME J. Fluids Eng.* **1989**, *111*, 387.
9. Yoshihara, Y.; Ikegami, M.; Mine, N. *Trans. Japan Soc. Mech. Eng., Series B* **1990**, *56*, 845.
10. Yoshihara, Y.; Tanaka, T. *Trans. Japan Soc. Mech. Eng. Series B* **1995**, *61*, 408.
11. Miller, J. A.; Bowman, C. T. *Prog. Energy Combust. Sci.* **1989**, *15*, 287.
12. Higashihara, T.; Gardiner, W. C., Jr.; Hwang, S. M. *J. Phys. Chem.* **1987**, *91*, 1900.
13. Klatt, M.; Spindler, B.; Wagner, H. G. *Z. Phys. Chem.* **1995**, *191*, 241.
14. Votsmeier, M.; Song, S.; Davidson, D. F.; Hanson, R. K. *Int. J. Chem. Kinet.* **1999**, *31*, 323.
15. Hwang, S. M.; Higashihara, T.; Shin, K. S.; Gardiner, W. C., Jr. *J. Phys. Chem.* **1990**, *94*, 2883.
16. Lifshitz, A.; Bidani, M.; Carroll, H. F.; Hwang, S. M.; Fu, P. Y.; Shin, K. S.; Gardiner, W. C., Jr. *Combustion and Flame* **1991**, *86*, 229.
17. Katak, M. V.; Manrique, K. S. De.; Aglave, R. H.; Hesketh, R. P. *Combustion and Flame* **1997**, *108*, 235.
18. GRI-Mechanism 3.0 is available by World Wide Web using the http://euler.berkeley.edu/gri_mech/version30/text30.html, 1999.
19. Coda Zabetta, E.; Kilpinen, P.; Hupa, M.; Stahl, K.; Leppalahti, J.; Cannon, M.; Nieminen, J. *Energy & Fuels* **2000**, *14*, 751.
20. Dean, A. M.; Bozzelli, J. W. In *Gas-Phase Combustion Chemistry*; Gardiner, W. C., Jr., Ed.; Springer-Verlag: New York, 2000; p 125.
21. Kee, R. J.; Rupley, F. M.; Miller, J. A. *The Chemkin Thermodynamic Data base* Sandia National Laboratories Report SAND87-8215B; 1990.
22. Kee, R. J.; Rupley, F. M.; Meeks, E.; Miller, J. A. *Chemkin-III; A Fortran Chemical Kinetics Package for the Analysis of Gas-Phase Chemical and Plasma Kinetics*, Sandia National Laboratories Report SAND96-8216; 1996.
23. Lutz, A. E.; Kee, R. J.; Miller, J. A. Sandia National Laboratories Report NO. SAND87-8248; 1991.
24. Jee, S. B.; Kim, W. K.; Shin, K. S. *J. Korean Chem. Soc.* **1999**, *43*, 156.
25. Jee, S. B.; Kim, K. Y.; Shin, K. S. *Bull. Korean Chem. Soc.* **2000**, *21*, 1015.
26. Kim, W. K.; Shin, K. S. *J. Korean Chem. Soc.* **1997**, *41*, 600.
27. Tsang, W.; Lifshitz, A. *Annual Review of Physical Chemistry* **1990**, *41*, 559.
28. Jee, S. B.; Kim, W. K.; Shin, K. S. *J. Korean Chem. Soc.* **1999**, *43*, 156.
29. Shim, S. B.; Jeong, S. H.; Shin, K. S. *J. Korean Chem. Soc.* **1998**, *42*, 575.
30. Kim, K. Y.; Shin, K. S. *Bull. Korean Chem. Soc.* **2001**, *22*, 303.
31. Lissianski, V. V.; Zamansky, V. M.; Gardiner, W. C., Jr. In *Gas-Phase Combustion Chemistry*; Gardiner, W. C., Jr., Ed.; Springer-Verlag: New York, 2000; p 1.